Electronic Supporting Information:

Self-Assembled 3D Free-Standing Superlattice of Gold Nanoparticles Driven by Interfacial Instability of Emulsion Droplets

Xuejie Liu,[a,b] Xuan Yue,[a,b] Nan Yan*[a] and Wei Jiang*[a,b]

[a] State Key Laboratory of Polymer Physics and Chemistry, Changchun Institute of Applied Chemistry, Chinese Academy of Sciences, Changchun 130022, China.

E-mail: nyan@ciac.ac.cn; wjiang@ciac.ac.cn.

[b] University of Science and Technology of China, Hefei 230026, China.

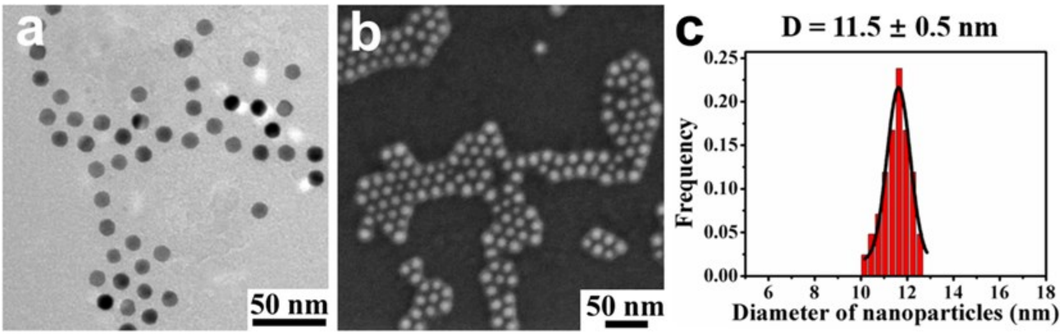

Fig. S1 TEM (a) and the corresponding SEM (b) images of the monodispersed AuNPs@PS_{2k}/$P2VP_{2.5k}$ building blocks obtained by seed-mediated growth method and the followed surface modification with PS-SH and P2VP-SH homopolymers. (c) The size distribution histogram of the synthesized AuNPs@PS_{2k}/$P2VP_{2.5k}$ building blocks.

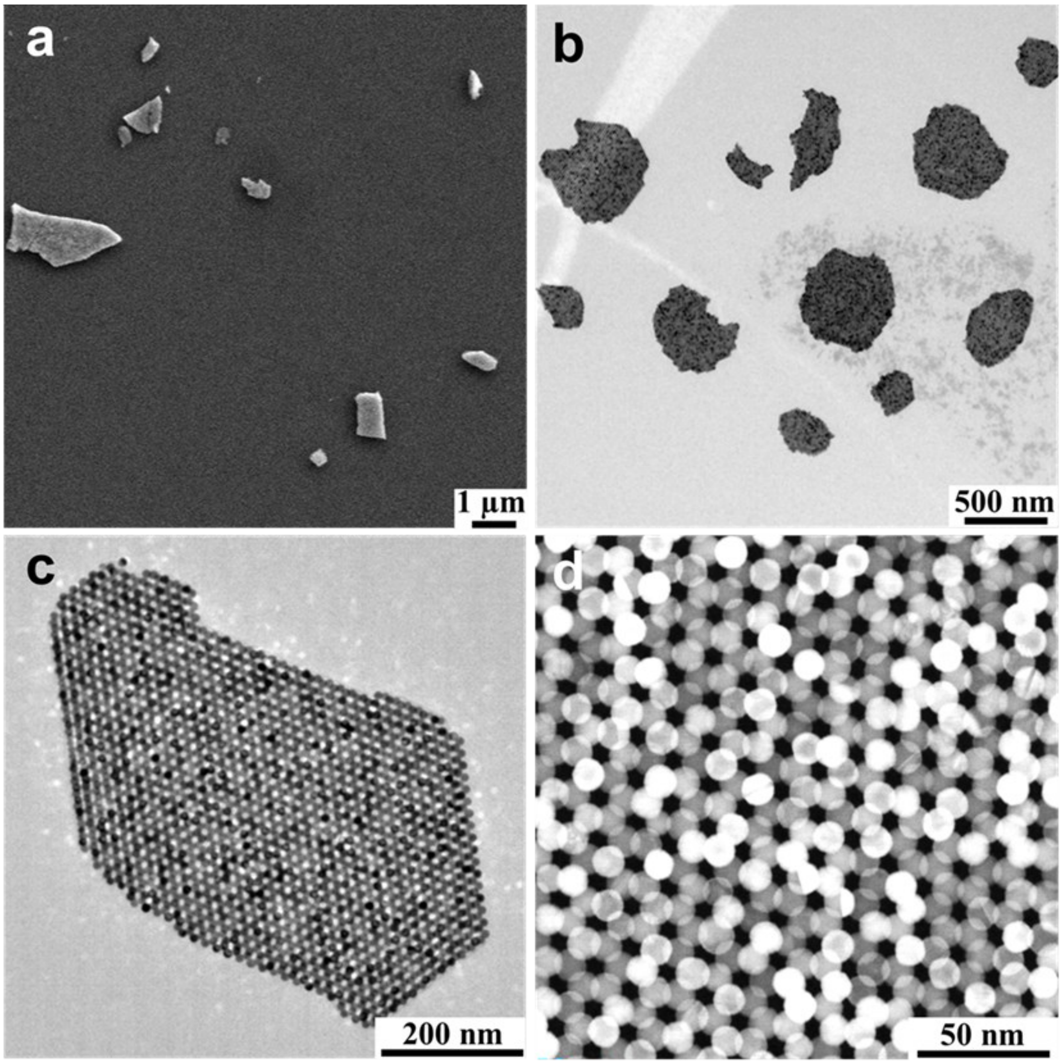

Fig. S2 SEM (a) and TEM (b) images of the fabricated 3D organic/inorganic AuNP superlattice sheets under low magnification. (c) The magnified TEM image of a single superlattice sheet. (d) The high-magnified STEM image of the 3D superlattice, indicating that the AuNPs@PS_{2k}/$P2VP_{2.5k}$ building blocks present highly ordered configuration within the 3D superlattice.

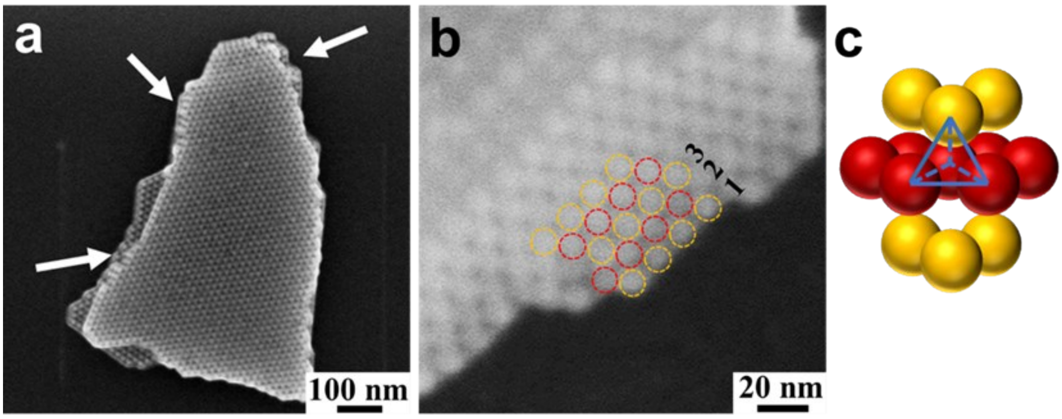

Fig. S3 The multilayer stacked arrangement of the 3D free-standing superlattice. (a) SEM image of a superlattice sheet at low magnification. (b) Magnified SEM image of the edge of the superlattice structure showing that the self-assembled superlattice sheet is multilayer and the AuNP building blocks arrange in a tetrahedron. AuNP building blocks in adjacent layers are arranged directly above the center of equilateral triangle produced by nanoparticles at the three corners in the neighboring layers. (c) The proposed model of the arrangement and configuration of the AuNPs@PS_{2k}/$P2VP_{2.5k}$ building blocks in the multilayer 3D superlattice sheet.

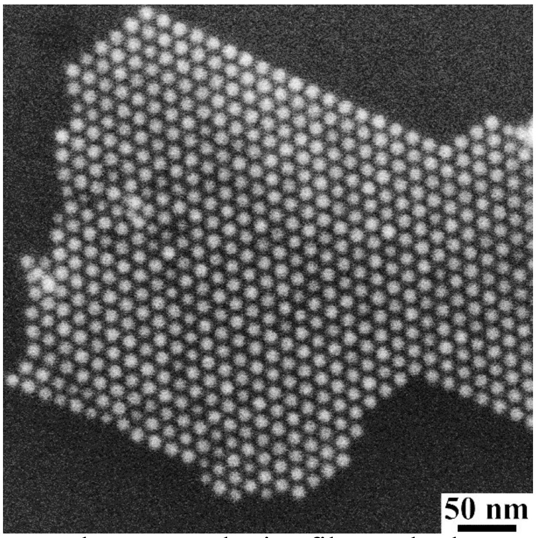

Fig. S4 SEM image of the monolayer superlattice film under low magnification.

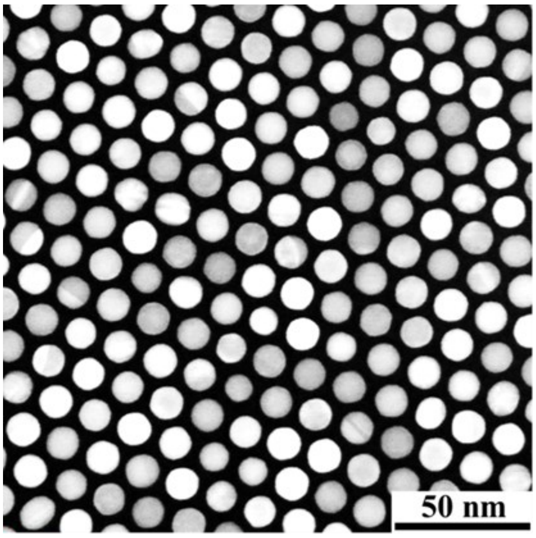

Fig. S5 STEM image of the monolayer superlattice film showing that the AuNPs@PS_{2k}/$P2VP_{2.5k}$ building blocks present a standard hexagonal packing.

Fig. S6 OM images demonstrating the spontaneous permeation of aqueous phase into the emulsion droplets and the deformation of emulsion droplets with the evaporation of chloroform. The initial stage (*i.e.*, 0 min) shows that the initial homogeneous emulsion droplets are spherical. With the volatilization of chloroform, the homogeneous spherical emulsion droplets are gradually permeated by surfactant aqueous solution (*i.e.*, 2 min). Eventually, the spherical emulsion droplets spontaneously break up into flat droplets due to the excessive penetration of the external aqueous solution (*i.e.*, 6 min).

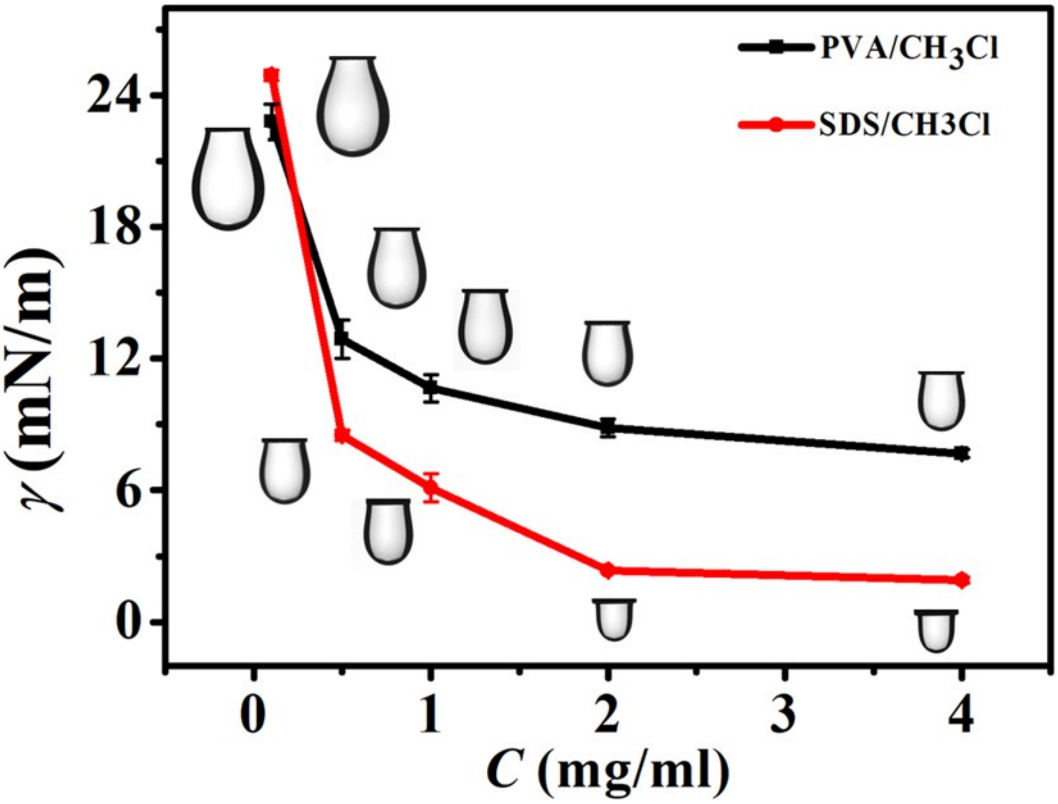

Fig. S7 Plot of interfacial intension at the interface between water and pure chloroform as a function of C_{SDS} and C_{PVA}. The interfacial intension is measured *via* pendant drop tensiometry. The insets are the images of droplets used to determine the interfacial intension.

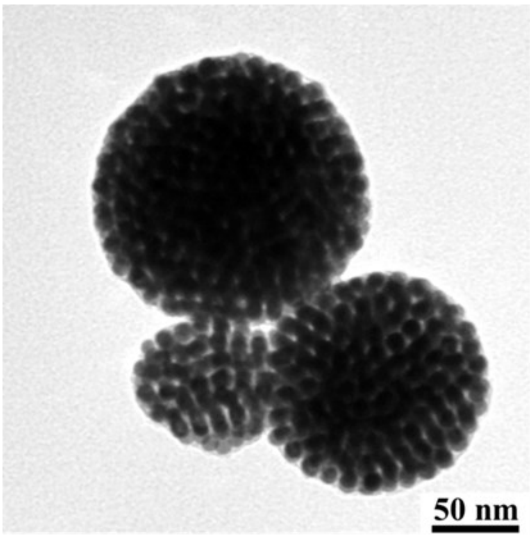

Fig. S8 TEM image of the obtained spherical assemblies at C_{SDS} = 0.1 mg mL^{-1}.

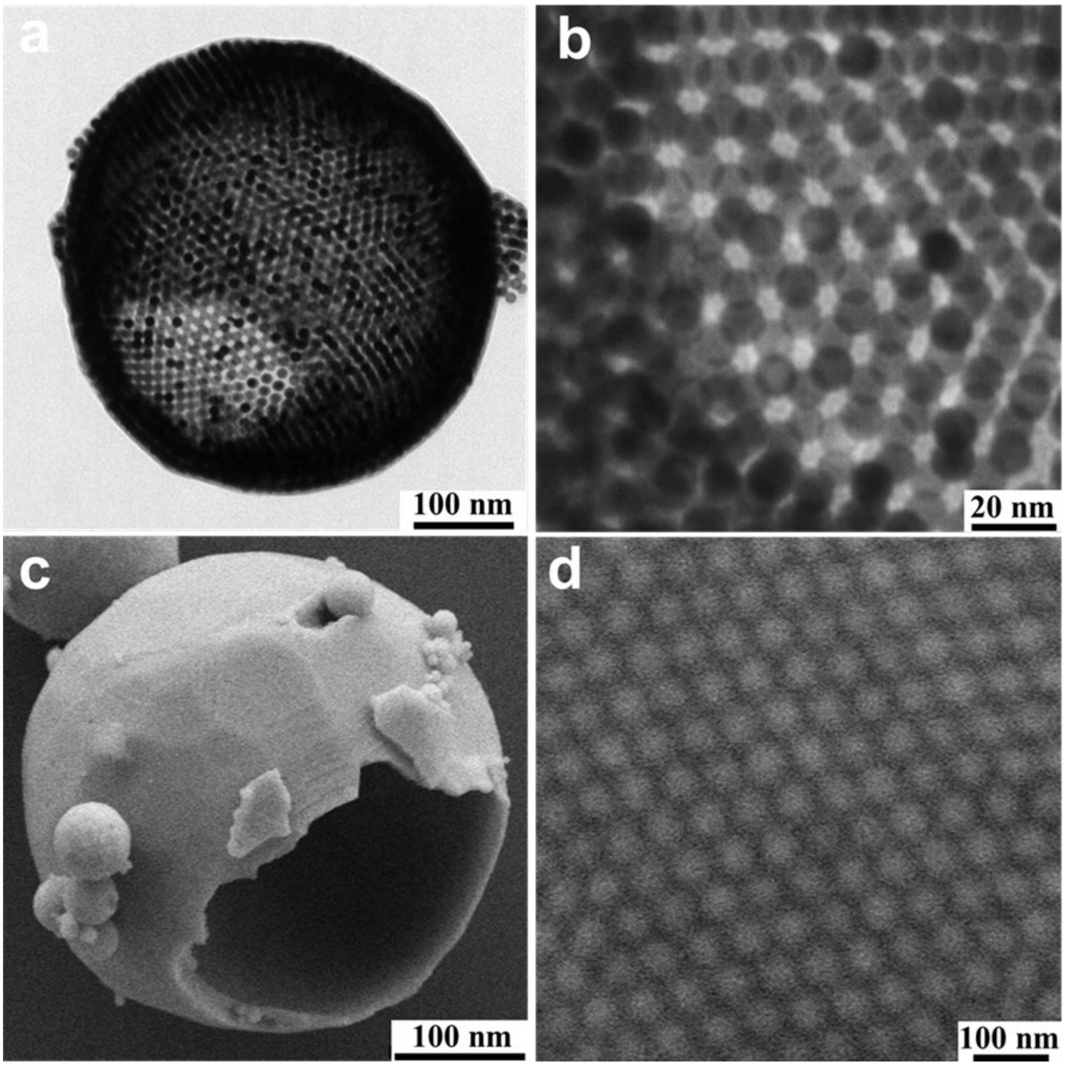

Fig. S9 TEM (a, b) and SEM (c, d) images of the obtained vesicles at C_{SDS} = 2.0 mg mL^{-1} under different magnification.

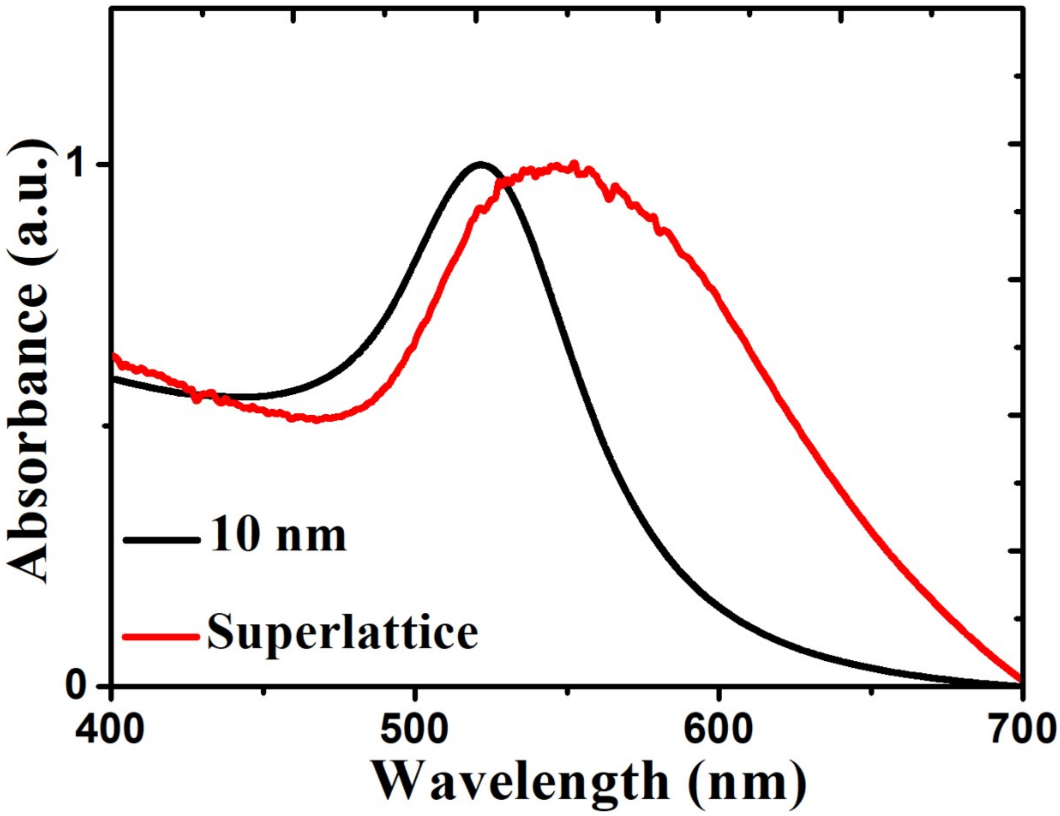

Fig. S10 UV-vis spectrums of the AuNP building blocks (black line) and the self-assembled superlattice (red line).

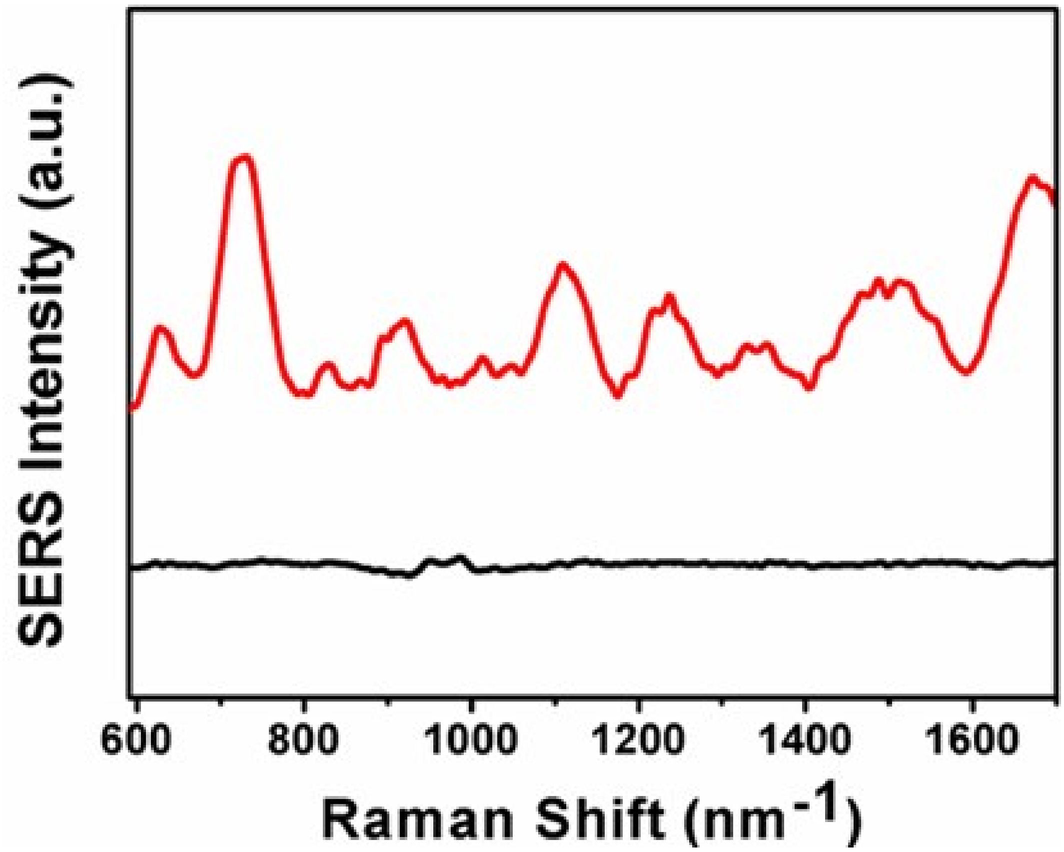

Fig. S11 Raman scattering spectra of Rhodamine 6G on the AuNPs@PS_{2k}/$P2VP_{2.5k}$ building blocks before the hierarchical assembly (black line) and highly ordered superlattice (red line) substrates.